ISSN 1023-1935, Russian Journal of Electrochemistry, 2019, Vol. 55, No. 11, pp. 1136–1143. © Pleiades Publishing, Ltd., 2019.
Published in Russian in Elektrokhimiya, 2019, Vol. 55, No. 11, pp. 1391–1399.

Testing Reactivity Descriptors for the Electrocatalytic Activity of OPG Hybrid Electrodes Modified with Iron Macrocyclic Complexes and MWCNTs for the Oxidation of Reduced Glutathione in Basic Medium[1]

C. Gutiérrez-Cerón[a], *, N. Silva[b], I. Ponce[a], and J. H. Zagal[a], **

[a] *Laboratorio de Electrocatalysis, Departamento de Química de los Materiales, Facultad de Química y Biología, Universidad de Santiago de Chile, Sucursal Matucana, Santiago, 9170022 Chile*

[b] *Facultad de Diseño, Universidad del Desarrollo, Las Condes, Santiago, Chile*

**e-mail: cristian.gutierrezce@usach.cl*

***e-mail: jose.zagal@usach.cl*

Received April 2, 2019; revised June 15, 2019; accepted July 11, 2019

Abstract—In this work we have tested the Fe(III)/(II) redox potential of the catalysts as a reactivity descriptors of iron macrocyclic complexes (FeN4) adsorbed on multi-walled carbon nanotubes (MWCNTs) and deposited on ordinary pyrolytic graphite (OPG). The reaction examined is the oxidation of glutathione (GSH) a biologically important molecule. The experiments were conducted in 0.1 M NaOH and kinetic measurements were performed on MWCNT previously modified with FeN4 macrocycle complexes. This modified FeN4–MWCNTs were deposited on pristine OPG electrodes. From previous work it is known that for FeN4 complexes directly adsorbed on OPG, the activity as $(\log i)_E$ plotted versus the Fe(II)/(I) redox potential follows a volcano correlation for the oxidation of glutathione. We wanted to test these correlations on hybrid electrodes containing MWCNTs and essentially the carbon nanotubes have no influence in these correlations and the redox potentials a are good reactivity descriptors, regardless of the way the FeN4 catalysts are attached to the electrode. Further, we find volcano correlations when using the Fe(II)/(I) and the Fe(III)/(II) redox potentials as reactivity descriptors. The volcano correlation when using the Fe(III)/(II) redox potential exhibits a maximum at $E^\circ = -0.26$ V vs SCE which is close to the potential for comparing the different activities. This interesting result seems to indicate that the maximum cannot be explained only in terms of the Sabatier principle where θ_{RS}, the surface coverage of adsorbed intermediate is close to 0.5 but instead to a surface coverage of active sites $\theta_{Fe(II)}$ equal to 0.5, which occurs at the Fe(III)/(II) formal potential.

Keywords: glutathione oxidation, Fe phthalocyanines, Fe porphyrins, volcano correlations, reactivity descriptors

DOI: 10.1134/S1023193519110077

INTRODUCTION

Glutathione (GSH) is an electrochemically reactive biological molecule than can undergo the disulfide (GSSG)/thiol (GSH) redox process [1–4]. This process is very important in biological systems. In living systems glutathione exists in both reduced (GSH) and oxidized (GSSG) states [4]. In the reduced state, the thiol group of cysteine can donate a reducing equivalent ($H^+ + e^-$) to other molecules, such as reactive oxygen species to neutralize them, or to protein l-cysteines to maintain their reduced forms. When donating an electron, glutathione itself becomes reactive and readily reacts with another reactive glutathione to form glutathione disulfide (GSSG). Glutathione is active electrochemically and can be electrooxidized to the corresponding disulfide [4–15]. In previous work, we have found that MN4 macrocyclic complexes, when adsorbed or anchored on carbon surfaces catalyze the oxidation of several thiols, including glutathione [4, 8–25]. We have established that the M(II)/(I) redox potential is a reactivity descriptor for this reaction and the reactivity of these molecules varies in a non-linear fashion with the M(II)/(I) redox potential, giving volcano correlations. These volcano correlations are well known for metal electrodes but less known for molecular catalysts like MN4 complexes. In previous work we have found that for the oxidation of glutathione catalyzed by MN4 macrocyclic complexes adsorbed on ordinary pyrolytic graphite [8], the reactivity trends are essentially the same as those found for the oxidation of other thiols [8–25]. The differences observed are essentially

[1] This paper is dedicated to the 80th anniversary of Professor V.V. Malev who has made a considerable contribution into modern directions of electrochemistry.

the position of the maximum of the volcano, which, according to the Sabatier principle corresponds to an interaction of the reacting molecule with the active site that is not too strong, not too weak. The maximum in the volcano would correspond to a free energy of adsorption of the reacting molecule $\Delta G^{o}_{ad} = 0$, which corresponds to a situation where half of the surface is covered with adsorbed intermediates. On the other hand, carbon nanotubes have been used by many authors as interesting platforms to produce hybrid electrodes that can have applications in electrocatalysis and electroanalysis. Some authors have suggested that carbon nanotubes themselves have catalytic activity. The latter will depend on the functionalities present on these nanotubes. In this work we wanted to test the reactivity descriptors for Fe phthalocyanines (FePcs) and Fe porphyrins (FePs) attached to the external walls of CNTs for the oxidation of glutathione.

EXPERIMENTAL

Materials

Multi-walled carbon nanotubes (MWCNTs) were acquired from DropSens. Approximate dimensions are 10 nm (diameter) and 1–2 μm (length) bearing COOH groups (approx. 5% functionalization). The iron phthalocyanines (FePcs), Fe perchlorinated phthalocyanine (16(Cl)FePc), Fe phthalocyanine (FePc) were obtained from Aldrich and used as provided. Fe tetrasulfonated phthalocyanine ($4\beta(SO_3^-)$FePc) and Fe octakis (hydroxyethylthio) phthalocyanine ($8\beta(SC_2H_4OH)$FePc was synthesized according to the method described in the literature [26]. Fe tetranitrophthalocyanine ($4\beta(NO_2)$FePc) and Fe tetraaminophthalocyanine ($4\beta(NH_2)$FePc) were obtained from Midcentury Chemicals, Posen, IL. Fe tetraphenyl porphyrin (4(Ph)FeP), Fe octaethyl porphyrin (8(Et)FeP), Fe tetra(4-methoxyphenyl) porphyrin ($4(PhOCH_3)$FeP), Fe (4-sulfonatophenyl) porphyrin ($4(PhSO_3^-)$FeP, Fe tetra(4-pyridyl) porphyrin (4(4-Py)FeP) and Fe tetra(N-methyl-4-pyridyl) porphyrin chloride 4(4-Py(N-CH_3))FeP were obtained from Aldrich and used as provided. Electrolytic solutions were prepared from deionized, bidistilled water, and O_2 was removed with ultra-pure N_2 gas. NaOH was of analytical grade from Merck and used without further purification. Dimethylformamide was of spectroscopic grade from Aldrich and used as provided. Reduced glutathione (GSH) was obtained from Merck. All the other chemicals were of analytical grade.

Electrochemical Measurements

The working electrode (Pine Instruments) was an ordinary pyrolytic graphite disk (OPG), with a geometrical area of 0.196 cm^2 mounted in Teflon. Current densities for OPG electrodes were estimated using the geometric area. For OPG electrodes coated with carbon nanotubes, current densities were estimated considering an increase in the roughness of the electrode by the presence of the CNTs of 60%. A saturated calomel electrode (SCE) and platinum (99.99% Aldrich spiral wire exposing an area of 14 cm^2) were used as the reference and auxiliary electrodes, respectively. A conventional Pyrex glass cell of three compartments was employed, with the reference electrode compartment connected to the main compartment by a Luggin capillary. Cyclic voltammogram (CV) and linear sweep voltammetry (LSV) measurements were conducted on a BAS CV-100B Voltammetric Analyzer. All measurements were carried out in 0.1 M NaOH at 25 ± 1°C and purged with ultra-pure N_2 gas during 30 min.

Preparation of Modified Electrode with Fe Phthalocyanines and Fe Porphyrins (FePs)

The OPG electrode was polished before each experiment with 800 and 1200 grit emery paper and 1 μm alumina followed by ultrasonic treatment in purified water for 2 min. Adsorption of FePcs and FePs was achieved by placing a drop of a 10^{-4} M solution of a given complex on the electrode surface. Dimethylformamide (DMF) was used to prepare all the complex solutions except for $4\beta(SO_3^-)$FePc and $4(PhSO_3^-)$FeP which were dissolved in water. To avoid the formation of precipitates or microcrystals on the graphite, the electrode was rinsed with the corresponding solvent, and then, the excess of organic solvent was eliminated with ethanol before rinsing with bidistilled water.

Preparation of Hybrid MWCNT + FePcs and MWCNT + FePs Electrodes

MWCNTs were dispersed in solutions of either phthalocyanines or porphyrins (1 mg mL^{-1}) by sonication for 30 min. The dispersions were left to rest for 24 h at room temperature. After that, they were filtered and washed with DMF and ethanol to remove any excess of complexes that were not adsorbed on the surface of the nanotubes. The solid obtained was allowed to dry in an oven at 40°C for 24 h. A new suspension was then obtained from the filtered MWCNT + FePcs or MWCNT + FePs (1 mg mL^{-1} in DMF) and used for subsequent modification of the OPG electrode surface previously polished. The same procedure was utilized to prepare MWCNT+ $4\beta(SO_3^-)$FePc and $4(PhSO_3^-)$FeP but using bidistilled water.

RESULTS AND DISCUSSION

Figure 1 shows typical cyclic voltammograms for a series of FeN4 complexes adsorbed on MWCNTs. Two distinct redox signals are observed. Peak labeled 1 corresponds to the metal centered Fe(II)/(I) reversible

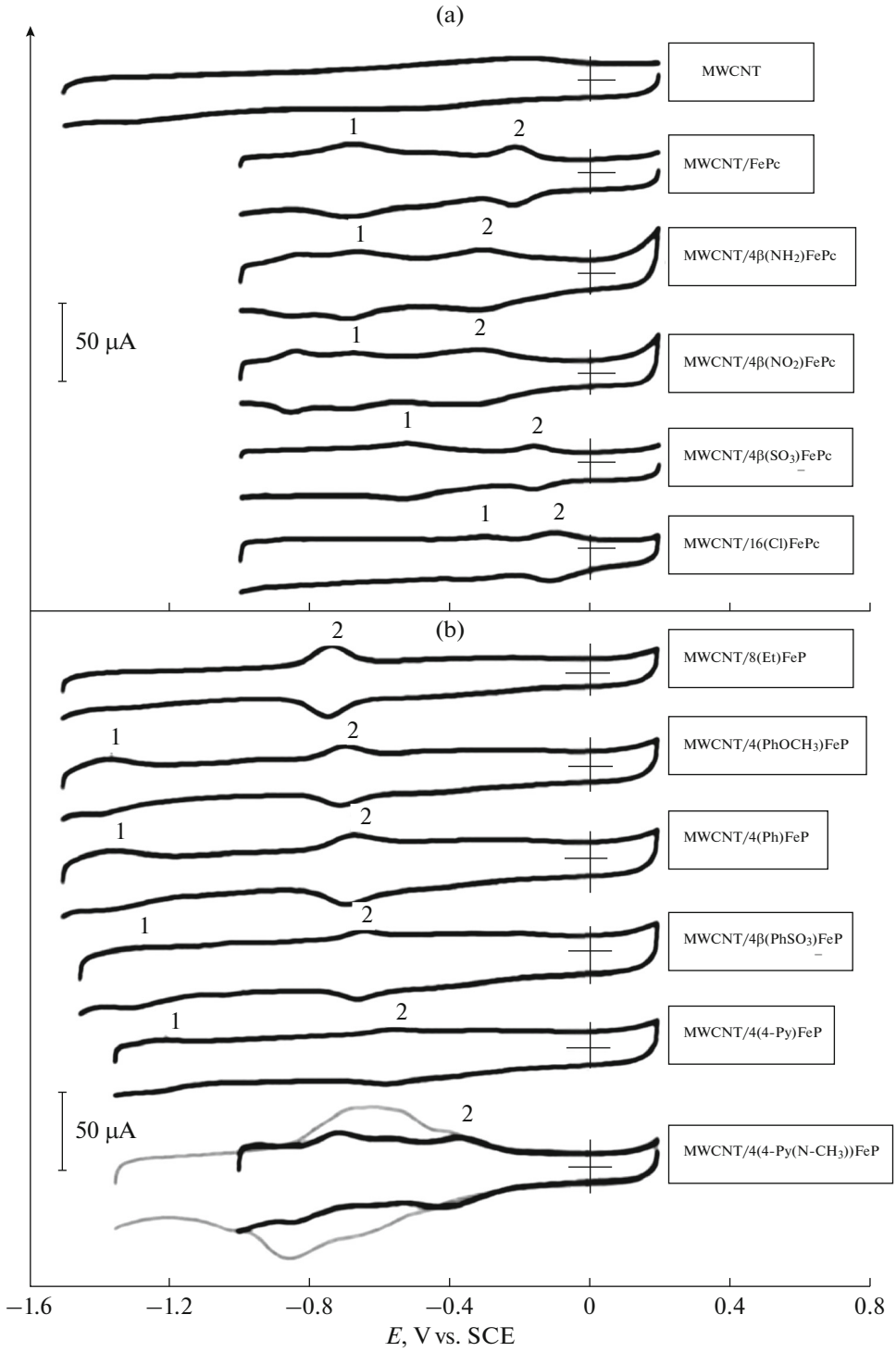

Fig. 1. Cyclic voltammograms of OPG electrodes modified with MWCNT/FePcs (a) and MWCNT/FePs (b) in 0.1 M NaOH aqueous solution. Scan rate = 0.1 V s^{-1}.

redox transition occurring on the immobilized FeN4 complexes and peak 2 to the corresponding Fe(III)/(II) process. These processes have been characterized in previous work [8]. Both redox processes shift to more positive potentials as the electron-withdrawing power of the ligand increases. By using the same metal and changing the ligand it is possible to modify the redox potentials in a wide range of values, since depending on of electron-withdrawing power of groups located on the ligand will be possible to shift the redox process.

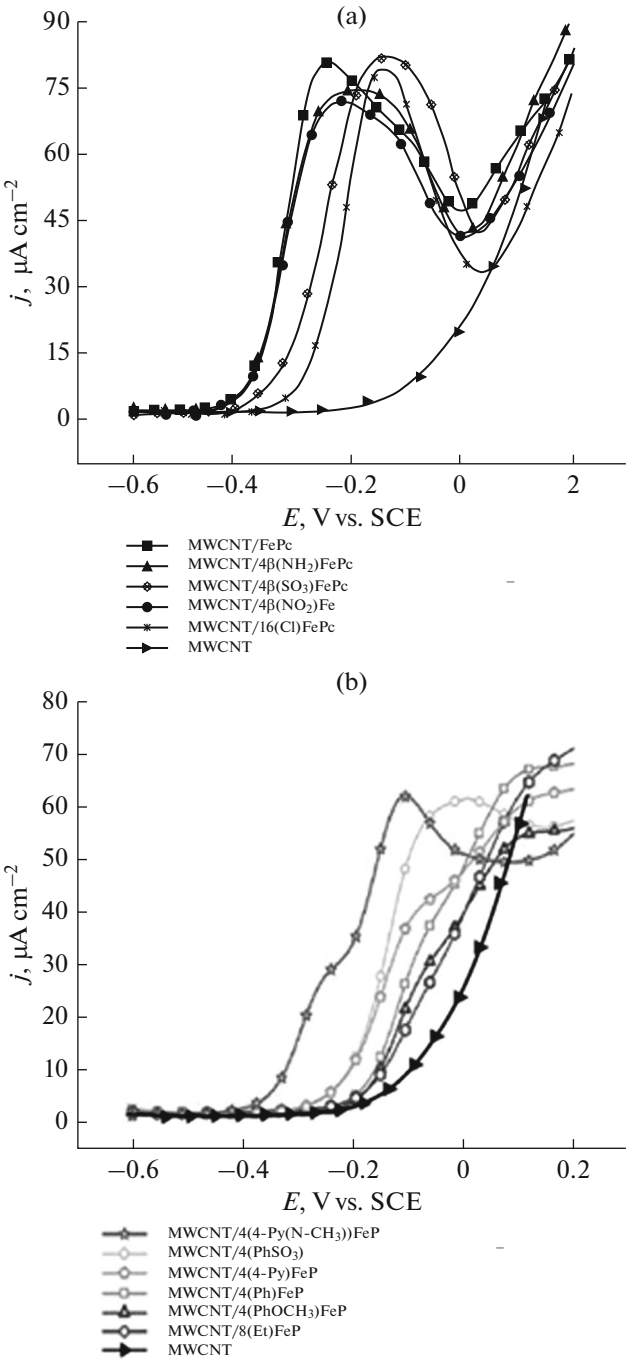

Fig. 2. Polarization curves of the oxidation of 5 mM GSH in 0.1 M NaOH aqueous solution on various hybrid OPG electrodes modified with (a) MWCNT/FePcs and (b) MWCNT/FePs. Scan rate = 0.002 V s^{-1}.

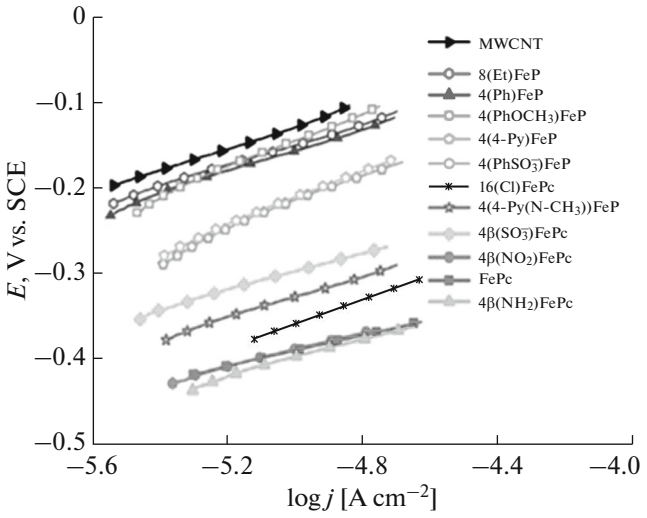

Fig. 3. Tafel plots for the oxidation of GSH on MWCNT/FePcs and MWCNT/FePs adsorbed on OPG. Data obtained from polarization curves in Fig. 2.

For example electron with drawings groups located on the ligand will shift the redox potentials to more positive values. It is possible then to test the redox potentials as a reactivity descriptor for the oxidation of glutathione and for many other reactions [8, 11, 16, 21–25, 27–38].

Figure 2 shows a series of polarization curves obtained with a rotating disk OPG electrodes coated with MWCNTs modified with different FeN4 molecular catalysts. It is clear from the figure that the reactivity is dictated by the nature of each FeN_4 complex. The OPG/MWCNT electrode without any Fe complexes present on the interface shows very low activity indicating that this electrode provides no or very limited active sites for glutathione to adsorb and react. When comparing Fig. 2a with 2b, Fe phthalocyanines show much higher activity than Fe porphyrins and this can be attributed to the fact that in general Fe porphyrins exhibit Fe(III)/(II) too negative compared to those of Fe phthalocyanines. It is important to point out that Fe(II) is the active site and Fe(III) is inactive due to the process $Fe(II) + OH^- \rightleftarrows Fe(III)OH + e$. Even if Fe(III) were active GS^- does not seem to compete with OH^- so essentially the Fe(III) sites are occupied and inactive for glutathione oxidation. So if the formal potential of the $Fe(II) + OH^- \rightleftarrows Fe(III)OH + e$ reaction for a given FeN4 complex occurs at potentials close or more negative than the onset for oxidation of glutathione, as the potential is scanned to more positive potentials, for those particular complexes the surface becomes rapidly deprived of Fe(II) active sites which could be similar to state that the active sites become gradually poisoned by OH^- as Fe(II) loses an electron and goes to Fe(III). This analysis is corroborated by the experimental observation that the MWCNT/8(Et)FeP catalyst exhibits the most negative Fe(III)/(II) redox potential and shows the lowest activity of all hybrid catalysts (see polarization curves in Fig. 2 and Tafel plots in Fig. 3). To test this any further we have compared the activities of all different catalysts at constant potential versus the Fe(II)/(I) redox potential in the volcano correlation of Fig. 4. We have used the Fe(II)/(I) redox process as in homoge-

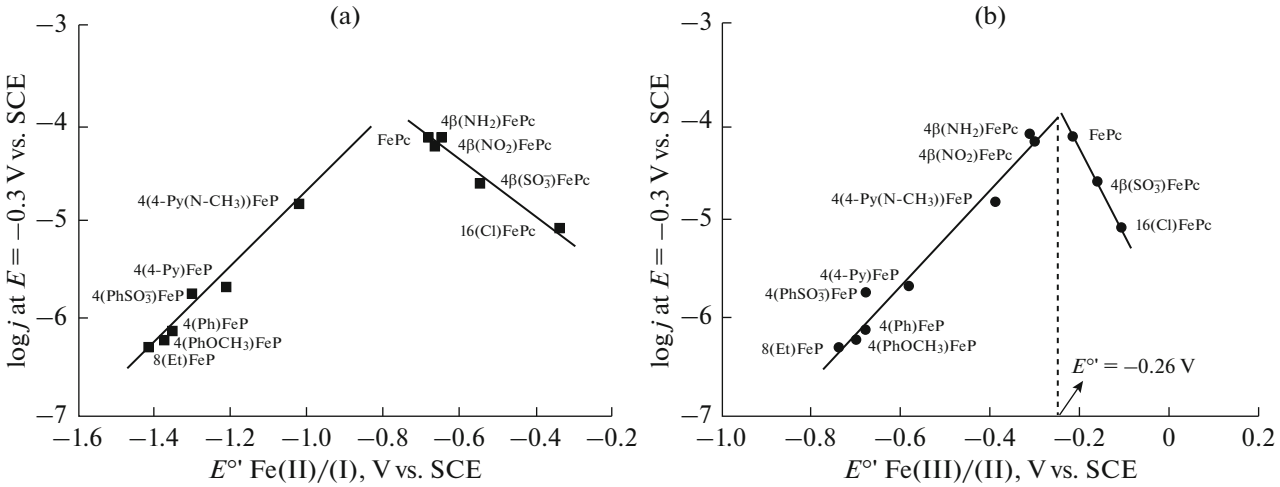

Fig. 4. Volcano plots of log j (at E = –0.3 V vs. SCE) vs. $E^{\circ'}$ Fe(II)/(I) and $E^{\circ'}$ Fe(III)/(II) of MWCNT/FePcs and MWCNT/FePs adsorbed on OPG for the oxidation of 5 mM of GSH in 0.1 M NaOH.

neous phase several thiols reduce the Fe(II) to Fe(I) and this has been corroborated by in situ UV-vis spectra and epr spectroscopy [19, 39, 40].

Proposed ET Mechanism

For the oxidation of glutathione catalyzed by FeN4 complexes adsorbed on OPG/MWCNT, the Tafel slopes are similar. The kinetic parameters do not depend on the type of FeN4 complex so a common mechanism can be proposed for the oxidation of glutathione catalyzed by the different Fe macrocyclics. GSH corresponds to the protonated glutathione molecule. This mechanism is essentially similar to that reported before for the oxidation of glutathione catalyzed by FeN4 complexes directly adsorbed on OPG [8]:

$$GSH_{(aq)} + OH^- \leftrightarrows GS^-_{(aq)} + H_2O, \quad (1)$$

$$GS^-_{(aq)} + [Fe(II)Pc]_{ads} \leftrightarrows [RS{-}Fe(II)Pc]_{ads} + e \quad (2)$$
$$\Delta G_{ads},$$

$$[GS{-}Fe(II)Pc]_{ads} + OH^- \rightarrow [Fe(II)Pc]_{ads} + GS\bullet + H_2O + e, \quad (3)$$

$$2\,GS\bullet \rightarrow GSSG \quad \text{fast.} \quad (4)$$

In our case the pH is higher than the pK_a of glutathione (pK_a = 8.66, [7]) so equilibrium (1) is practically shifted to the right. The total concentration of dissociated glutathione $[GS^-]_{aq}$ (see Eq. (1)) is then equal to the total concentration of glutathione in the electrolyte. The final product of the oxidation process is the glutathione disulfide (GSSG) and the active site is the Fe(II) metal center in the complex [8]. The rate of the reaction can be derived as in a previous manuscript for the oxidation of cysteamine [27]. One can assume that the surface concentration of the intermediate adduct $[Fe(II){-}GS]_{ads}$ is under steady state conditions. According to the reactions scheme one can assume that the chemical order in OH^- of one first and a first order in the fraction of occupied sites $\theta_{[RS-Fe(II)]}$:

$$j = nFk_r(E, \Delta G_{ads})\left[OH^-\right]\theta_{[RS-Fe(II)]}. \quad (5)$$

The details about this derivation can be found in previous work [32]. The fraction of Fe centers in the active state Fe(II) is given by the Nernst equation applied to surface confined species, and assuming ideal behaviour. $\theta_{[Fe(II)]}$ is the potential–dependent fraction of catalytic sites in the active state Fe(II):

$$\theta_{[Fe(II)]} = \frac{\exp\left(F\left(E - E^{\circ}_{\frac{II}{I}}\right)\right)}{1+\exp\left(F\left(E - E^{\circ}_{\frac{II}{I}}\right)\right)}\frac{1}{1+\exp\left(F\left(E - E^{\circ}_{\frac{III}{II}}\right)\right)}. \quad (6)$$

ΔG_{ads} is the free energy of step (2), k_{ads} and k_{des} are the adsorption and desorption rate constants of step 2, and k_r is the rate constant of step 3. $\theta_{[Fe(II)]}$ is equal to unity at $E^{\circ}_{Fe(II)/(I)} < E < E^{\circ}_{Fe(III)/(II)}$ and essentially zero 0.1 V bellow $E^{\circ}_{Fe(II)/(I)}$ and 0.1 V above $E^{\circ}_{Fe(III)/(II)}$. This has been graphically demonstrated in [32].

The currents in polarization curves should decrease rapidly when E is above the $E^{\circ}_{Fe(III)/(II)}$, potential as the surface concentration of active Fe(II) sites decreases rapidly due to their oxidation to Fe(III), following Eq. (6). This is experimentally observed for the several cases studied in Fig. 2, especially Fe porphyrins. E°_2 is the standard equilibrium potential of step 2. We assume that Eq. (2), the electron transfer step follows the Butler–Volmer relationship with a symmetry factor α_i, and that all processes involving the adsorbed catalytic intermediate GS depend on ΔG_{ads} according to the Brønsted–Polanyi equation with a Brønsted

coefficients β_i. It can be assumed that the crossing of the energy barriers is symmetrical for the matter of simplicity. It this case the symmetry factor α_i and Brönsted coefficient β_i are all similar. For further simplicity it can be assumed that these coefficients are equal 0.5 so they can be labeled simply as α and β.

In previous work when studying the catalytic activity of a series of MN4 macrocyclics for the reduction of O_2 a linear correlation exists between ΔG_{ads}, the binding energies of M–O_2 and $E^{\circ}_{Fe(III)/(II)}$ [33]. We can then assume a linear correlation between the binding energy of the GS intermediate and the Fe(III)/(II) redox potential, $\Delta G_{ads} = -nFE^{\circ}_{FeIII/II} + C$ which indicates that a more positive $E^{\circ}_{Fe(III)/(II)}$ corresponds to a stronger binding energy of the GS intermediate. A similar correlation might exists for the Fe(II)/(I) since the separation between the Fe(II)/(I) and Fe(III)/(II) potentials is almost constant for the complexes studied The volcano correlation of Fig. 4b illustrates a plot $E^{\circ}_{Fe(III)/(II)}$ redox potential versus the activities as log i at constant potential. The currents for both weak and strong adsorption regions in the volcano correlation are then given by the following expressions:

$$(j_w)_E = nFk_w \exp\left(\beta FE^{\circ'}_{(III)/(II)}\Big/RT\right) \quad (7)$$

weak adsorption,

$$(j_s)_E = nFk_s \exp\left(-(1-\beta)FE^{\circ}_{(III)/(II)}\Big/RT\right) \quad (8)$$

strong adsorption.

These equations predict a rather symmetrical volcano correlation if β is equal to 0.5 and to a first approximation, agrees with the experimental data shown the volcano correlations of Fig. 4. Deviations from the symmetry might be attributed to deviations of β from 0.5.

It is important also to point out that for FeN4 complexes that have very negative Fe(III)/(II) redox potentials compared to E, the Fe(III)/(II) redox couple also influences the currents by lowering the fraction of catalytically active sites $\theta_{[Fe(II)]}$. $\theta_{[Fe(II)]}$ at $E = E$ can be estimated using Eq. (9).

Since Fe(III) binds OH^- rather strongly, these sites will be inactive for cysteine oxidation, leading to the observed inhibition at higher potentials (see Fig. 2). Essentially activity should be observed to a first approximation in the potential window $E^{\circ}_{Fe(II)/(I)} \le E \le E^{\circ}_{Fe(III)/(II)}$ and this agrees with the experimental results and was well those illustrated graphically in previous work [37]. The Tafel plots of Fig. 3 provide more information about the relative activities of the different complexes. The least active electrode is the one without any FeN4 complexes. The Tafel slopes are around 0.12 V/decade suggesting that step (2), the first one-electron transfer step is rate controlling. The activities in Fig. 4 are almost 10 times larger than those reported before for FeN4 complexes directly adsorbed on OPG [8] but the trends are the same so MWCNTs seem to only increase the area of the electrode without affecting the intrinsic activity of these complexes.

Finally, it is important to point out that the volcano correlation in Fig. 4b, when using Fe(III)/(II) redox potential as a descriptor, it exhibits a maximum at $E^{\circ} = -0.26$ V vs. SCE which is close to the electrode potential used for comparing the different activities. This interesting result seems to indicate that the maximum cannot be explained only in terms of the classical Sabatier principle where θ_{RS}, the surface coverage of adsorbed intermediate is hypothetically close to 0.5 but to a surface coverage of active sites $\theta_{Fe(II)}$ equal to 0.5, which occurs at the Fe(III)/(II) formal potential. So the falling of the currents when going from right to left in the volcano correlations could be due to a gradual decrease in $\theta_{Fe(II)}$ and not a gradual occupancy of active sites by RS_{ad} or to both effects combined. More experiments are required to clarify this point.

CONCLUSIONS

In this manuscript we have tested the metal-centered-redox potential of FeN4 complexes as reactivity descriptors for the oxidation of glutathione. We essentially have checked these reactivity trends when the complexes are deposited on multiwalled carbon nanotubes as it has been claimed by some authors that carbon nanotubes increase the activity of these complexes but this is primarily an area effect, unless specific functionalities are present on the carbon nanotubes that can act as axial ligands, and these ligands can modify the catalytic activity of metal complexes in general. In our case an increase in activity of ca. 10 times is observed by the presence of MWCNTs but this effect is practically the same for all FeN4 complexes and the trends in reactivity do not change by the presence of MWCNTs. The volcano correlations in Fig. 4 are essentially shifted by one order of magnitude with respect to the same trends observed for complexes directly adsorbed on OPG [8] and this is likely to be only an area effect but the essential features are maintained. This observation is very interesting since the redox potentials are reactivity predictors for these complexes regardless of the way they are attached to the electrode surface. These predictors then can be useful at the moment of designing high area electrodes containing these complexes for applications in sensors and electrocatalysis.

FUNDING

The authors are grateful to Fondecyt Projects 1140199, 1181037, Nucleo Milenio RC 120001 and Dicyt-Usach Postdoctoral Fellowship to C. G-C.

CONFLICT OF INTEREST

The authors declare that they have no conflict of interest.

REFERENCES

1. Meister, A., Glutathione metabolism and its selective modification, *J. Biol. Chem.,* 1988, vol. 263, p. 17205.
2. Meister, A. and Anderson, M.E., Glutathione, *Annu. Rev. Biochem.,* 1983, vol. 52, p. 711. https://doi.org/10.1146/annurev.bi.54.070183.003431
3. Ziegler, D.M., Role of reversible oxidation-reduction of enzyme thiols-disulfides in metabolic regulation, *Annu. Rev. Biochem.,* 1985, vol. 54, p. 305. https://doi.org/10.1146/annurev.bi.54.070185.001513
4. Sehlotho, N., Nyokong, T., Zagal, J.H., and Bedioui, F., Electrocatalysis of oxidation of 2-mercaptoethanol, l-cysteine and reduced glutathione by adsorbed and electrodeposited cobalt tetra phenoxypyrrole and tetra ethoxythiophene substituted phthalocyanines, *Electrochim. Acta,* 2006, vol. 51, p. 5125. https://doi.org/10.1016/j.electacta.2006.03.049
5. Masella, R. and Mazza, G., *Glutathione and Sulfur Amino Acids in Human Health and Disease,* New York: Wiley, 2009. https://doi.org/10.1002/9780470475973
6. Chakravarthi, S., Jessop, C.E., and Bulleid, N.J., The role of glutathione in disulphide bond formation and endoplasmic-reticulum generated oxidative stress, *EMBO Rep.,* 2006, vol. 7, p. 271. https://doi.org/10.1038/sj.embor.7400645
7. Tummanapelli, A.K. and Vasudevan, S., An initio MD simulation of the Brönsted acidity of glutathione in aqueous solutions: predicting pKa shifts of the cysteine residue, *J. Phys. Chem. B,* 2015, vol. 119, p. 15353. https://doi.org/10.1021/acs.jpcb.5b10093
8. Gutierrez, C., Paez, M., and Zagal, J.H., Reactivity descriptors for iron porphyrins and iron phthalocyanines as catalysts for the electrooxidation of reduced glutathione, *J. Solid State Electrochem.,* 2016, vol. 20, p. 3199. https://doi.org/10.1007/s10008-016-3396-z
9. Zagal, J.H., Aguirre, M.J., and Parodi, C.G., Electrocatalytic activity of vitamin B12 adsorbed on graphite electrode for the oxidation of cysteine and glutathione and the reduction of cystine, *J. Electroanal. Chem.,* 1994, vol. 374, p. 215.
10. Sekhosana, K.E., Antunes, E., Khene, S., D'Souza, S., and Nyokong, T., Fluorescence behavior of glutathione capped CdTe@ZnS quantum dots chemically coordinated to zinc octacarboxy phthalocyanines. *J. Lumin.,* 2013, vol. 136, p. 255. https://doi.org/10.1016/j.poly.2011.10.024
11. Porras Gutierrez, A., Rangel Argote, M., Griveau, S., Zagal, J.H., Gutierrez-Granados, S., Alatorre Ordaz, A., and Bedioui, F., Catalytic activity of electrode materials based on polypyrrole, multi-wall carbon nanotubes and Cobal phthalocyanine for the electrooxidation of glutathione and L-cysteine, *J. Chilean Chem. Soc.,* 2012, vol. 57, p. 1244. https://doi.org/10.4067/S0717-97072012000300010
12. Tang, H., Chen, J., Nie, J., Yao, S., and Kuang, Y., Electrochemical oxidation of glutathione at well-aligned carbon nanotube array electrode, *Electrochim. Acta,* 2006, vol. 51, p. 3046. https://doi.org/10.1016/j.electacta.2005.08.038
13. Safavi, A., Maleki, N., Farjami, E., and Mahyari, F.A., Simultaneous electrochemical determination of glutathione and glutathione disulfide at a nanoscale copper hydroxide composite carbon ionic liquid electrode, *Anal. Chem.,* 2009, vol. 81, p. 7538. https://doi.org/10.1021/ac900501j
14. Pereira-Rodrigues, N., Cofre, R., Zagal, J.H., and Bedioui, F., Electrocatalytic activity of CoPc adsorbed on graphite electrode for the oxidation of glutathione (GSH) and the reduction of its disulfide (GSSG) at physiological pH, *Bioelectrochemistry,* 2007, vol. 70, p. 147. https://doi.org/10/1016/j.bioelechem.2006.03.025
15. Sehlotho, N., Nyokong, T., Zagal, J.H., and Bedioui, F., Electrocatalysis of oxidation of 2-mercaptoethanol, L-cysteine and reduced glutathione by adsorbed and electro-deposited cobalt pyrrole-phenoxy and ethoxythiophene substituted phthalocyanines, *Electrochim. Acta*, 2006, vol. 51, p. 5125. https://doi.org/10.4067/S0717-97072012000300010
16. Griveau, S., Gulppi, M., Pavez, J., Zagal, J.H., and Bedioui, F., Cobalt phthalocyanine-based molecular materials for the electrocatalysis and electroanalysis of 2-mercaptoethanol, 2-mercaptoethanesulfonic acid, reduced glutathione and L-cysteine, *Electroanalysis*, 2003, vol. 15, p. 779. https://doi.org/10.1002/elan.200390096
17. Aguirre, M.J., Isaacs, M., Armijo, F., Bocchi, N., and Zagal, J.H., Catalytic electrooxidation of 2-mercaptoethanol on perchlorinated iron phthalocyanine adsorbed on graphite electrodes, *Electroanalysis,* 1998, vol. 10, p. 571. https://doi.org/10.1002/(SICI)1521-4109(199807)10:8<571:: AID-ELAN571>3.0.CO;2-7
18. Zagal, J.H. and Paez, C., Catalytic electrooxidation of 2-mercaptoethanol on a graphite electrode modified with metal phthalocyanines, *Electrochim. Acta,* 1989, vol. 34, p. 243.
19. Lezna, R.O., Juanto, S., and Zagal, J.H., Spectrochemical studies on tetrasulfonated metallophthalocyanines adsorbed on the basal plane electrode in the presence of cysteine, *J. Electroanal. Chem.,* 1998, vol. 452, p. 221. https://doi.org/10.1016/j.electacta.2013.07.230
20. Cárdenas-Jirón, G.I. and Zagal, J.H., Donor-acceptor intermolecular hardness on charge transfer reactions of substituted cobalt phthalocyanines, *J. Electroanal Chem.,* 2001, vol. 497, p. 55. https://doi.org/10.1016/S0022-0728(00)00434-4
21. Zagal, J.H. and Páez, C., Catalytic electro-oxidation of 2-mercaptoethanol on a graphite electrode modified with metal phthalocyanines, *Electrochim. Acta*, 1989, vol. 34, p. 243. https://doi.org/10.1016/0013-4686(89)87092-6
22. Cárdenas, G.I., Caro, C.A., Venegas-Yazigi, D., and Zagal, J.H., Theoretical study of charge transfer energy profile of cobalt phthalocyanine and 2-mercaptoethanol. Effect of the graphite on the global reactivity. *J. Molec. Struct. (Theochem.),* 2002, vol. 580, p. 193. https://doi.org/10.1016/S0166-1280(01)00613-3

23. Aguirre, M.J., Isaacs, M., Armijo, F., Basáez, L., and Zagal, J.H., Effect of the substituents on the ligand of iron phthalocyanines adsorbed on a graphite electrode on their activity for the electrooxidation 2-mercaptoethanol, *Electroanalysis*, 2002, vol. 14, p. 356. https://doi.org/10.1002/1521-4109(200203)14:5<356::AID-ELAN356>3.0.CO;2-U

24. Gulppi, M.A., Recio, F.J., Tasca, F., Ochoa, G., Silva, J.F., Pavez, J., and Zagal, J.H., Optimizing the reactivity of surface confined cobalt N4-macrocyclics for the electrocatalytic oxidation of L-cysteine by tuning the Co(II)/(I) formal potential of the catalyst, *Electrochim. Acta*, 2014, vol. 126, p. 37. https://doi.org/10.1016/j.electacta.2013.07.230

25. Silva, N., Castro-Castillo, C., Oyarzún, M.P., Ramírez, S., Gutierrez-Ceron, C., Marco, J.F., Silva, J.F., and Zagal, J.H., Modulation of the electrocatalytic activity of Fe phthalocyanine to carbon nanotubes: electrochemistry of l-cysteine and l-cystine, *Electrochim. Acta,* 2019, vol. 308, p. 295.

26. Akkurst, F. and Hamuryudan, E., Enhancement of solubility via esterification: synthesis and characterization of octakis (ester)-substituted phthalocyanines, *Dyes Pigments,* 2008, vol. 79, p. 153. https://doi.org/10.1016/j.dyepig.2008.02.001

27. Bedioui, F., Griveau, S., Nyokong, T., Appleby, A.J., Caro, C.A., Gulppi, M., Ochoa, G., and Zagal, J.H., Tuning the redox properties of metalloporphyrin and metallophthalocyanine based molecular electrodes for the highest electrocatalytic activity for the oxidation of thiols, *Phys. Chem. Chem. Phys.,* 2007, vol. 9, p. 3383. https://doi.org/10.1039/b618767f

28. Villagra, E., Bedioui, F., Nyokong, T., Canales, J.C., Páez, M.A., Costamagna, J., and Zagal, J.H., Tuning the redox properties of Co-N_4 macrocyclic complexes for the catalytic electrooxidation of glucose, *Electrochim. Acta*, 2008, vol. 53, p. 4883. https://doi.org/10.1016/j.electacta.2008.02.006

29. Linares-Flores, C., Zagal, J.H., Pavez, J., Pino-Riffo, D., and Arratia-Pérez, R., Reinterpreting the role of the catalyst formal potential. The case of thiocyanate electrooxidation catalyzed by CoN_4-macrocyclic complexes, *J. Phys. Chem. C,* 2012, vol. 116, p. 7091. https://doi.org/10.1021/jp300764n

30. Zagal, J.H., Cañete, P., Recio, J., Tasca, F., and Linares-Flores, C., Tuning the Fe(II)/(I) formal potential of FeN_4 catalysts adsorbed on graphite electrodes to the reversible potential of the reaction for maximum activity: hydrazine oxidation, *Electrochem. Comm.,* 2013, vol. 30, p. 34. https://doi.org/10.1016/j.elecom.2013.01.024

31. Silva, N., Castro-Castillo, C., Oyarzún, M.P., Ramírez, S., Gutierrez-Ceron, C., Marco, F.J., Silva, J.F., and Zagal, J.H., Modulation of the electrocatalytic activity of Fe phthalocyanine to carbon nanotubes: electrochemistry of l-cysteine and l-cystine, *Electrochim. Acta,* 2019, vol. 308, p. 295. https://doi.org/10.1016/j.electacta.2019.04.005

32. Silva, N., Calderón, S., Páez, M.A., Oyarzún, M.P., Koper, M.T.M., and Zagal, J.H., Probing the $Fe^{n+}/Fe^{(n-1)+}$ redox potential of Fe phthalocyanines as a reactivity descriptor in the electrochemical oxidation of cysteamine, *J. Electroanal. Chem.,* 2018, vol. 15, p. 502. https://doi.org/10.1016/j.jelechem.2017.12.068

33. Zagal, J.H. and Koper, M.K.T., Reactivity descriptors for the activity of MN_4 molecular catalysts for the oxygen reduction reaction, *Angew. Chem.,* 2016, vol. 55, p. 14510. https://doi.org/10.1002/anie.201604311

34. Linares, C., Geraldo, D., Paez, M., and Zagal, J.H., Non-linear correlations between the formal potential and Hammett parameters of substituted iron phthalocyanines and catalytic activity for the electrooxidation of hydrazine, *J. Sol. State Electrochem.,* 2003, vol. 7, p. 626.

35. Shumba, M. and Nyokong, T., Effects of covalent versus non-covalent interactions on the electrocatalytic behavior of tetracarboxyphenoxyphthalocyanine in the presence of multi-walled carbon nanotubes, *J. Coord. Chem.,* 2017, vol. 70, p. 1585. https://doi.org/10.1080/00958972.2017.1303679

36. O'Donoghue, C.S.J.N., Shumba, M., and Nyokong, T., Electrode modification through click chemistry using Ni and Co alkyne phthalocyanines for electrocatalytic detection of hydrazine, *Electroanalysis,* 2017, vol. 29, p. 1731. https://doi.org/10.1002/elan.201700084

37. Makinde, Z.O., Louzada, M., Mashazi, P., Nyokong, E.T., and Khene, S., Electrocatalytic behaviour of surface confined pentanethio cobalt(II) binuclear phthalocyanines towards the oxidation of 4-chlorophenol, *Appl. Surf. Sci.,* 2017, vol. 425, p. 702. https://doi.org/10.1016/j.apsusc.2017.06.271

38. Ureta-Zañartu, M.S., Alarcon, A., Muñoz, G., and Gutierrez, C., Electrooxidation of methanol and ethylene glicol on gold and on gold modified with an electrodeposited polyNiTSPc film, *Electrochim. Acta,* 2007, vol. 52, p. 7857. https://doi.org/10.1016/j.electacta.2007.06.055

39. Kaczmarzyk, T., Jacokski, T., and Dzilinski, K., Spectroscopic characteristic of Fe_I-phthalocyanine, *Nukleokina,* 2007, vol. 52, p. S99.

40. Bletsa, E., Solakidou, M., Louloudi, M., and Deligianakis, Y., Oxidative catalytic evolution of redox and spin-states of a Fe-phthalocyanine studied by EPR, *Chem. Phys Lett.,* 2016, vol. 649, p. 48.

41. Kobayashi, N., Shirai, H., and Hojo, N., Iron(III) phthalocyanines: oxidation and spin states of iron phthalocyanines with carboxyl groups, *Dalton Trans.,* 1984, vol. 10, p. 2107.